

Site-specific dissociation dynamics of ethylene at 157 nm: Atomic and molecular hydrogen elimination

Jim J. Lin, Chia C. Wang, Yuan T. Lee, and Xueming Yang

Citation: *The Journal of Chemical Physics* **113**, 9668 (2000); doi: 10.1063/1.1321044

View online: <http://dx.doi.org/10.1063/1.1321044>

View Table of Contents: <http://scitation.aip.org/content/aip/journal/jcp/113/21?ver=pdfcov>

Published by the [AIP Publishing](#)

Articles you may be interested in

[Molecular beam studies of the F atom reaction with propyne: Site specific reactivity](#)

J. Chem. Phys. **122**, 044307 (2005); 10.1063/1.1839865

[Dynamics of photodissociation of ethylene and its isotopomers at 157 nm: Branching ratios and kinetic-energy distributions](#)

J. Chem. Phys. **120**, 10983 (2004); 10.1063/1.1740711

[Site specificity in molecular hydrogen elimination from photodissociation of propane at 157 nm](#)

J. Chem. Phys. **111**, 1793 (1999); 10.1063/1.479507

[VUV photochemistry of CH₄ and isotopomers. I. Dynamics and dissociation pathway of the H/D-atom elimination channel](#)

J. Chem. Phys. **109**, 7105 (1998); 10.1063/1.477394

[Site and isotope effects on the molecular hydrogen elimination from ethylene at 157 nm excitation](#)

J. Chem. Phys. **109**, 2979 (1998); 10.1063/1.476888



Site-specific dissociation dynamics of ethylene at 157 nm: Atomic and molecular hydrogen elimination

Jim J. Lin

Institute of Atomic and Molecular Sciences, Academia Sinica, Taipei, Taiwan, Republic of China

Chia C. Wang

Department of Chemistry, National Taiwan University, Taipei, Taiwan, Republic of China

Yuan T. Lee

Institute of Atomic and Molecular Sciences, Academia Sinica and Department of Chemistry, National Taiwan University, Taipei, Taiwan, Republic of China

Xueming Yang^{a)}

Institute of Atomic and Molecular Sciences, Academia Sinica, Taipei and Department of Chemistry, National Tsing Hua University, Hsinchu, Taiwan, Republic of China

(Received 3 July 2000; accepted 8 September 2000)

The atomic and molecular hydrogen elimination processes from ethylene have been studied using a molecular beam apparatus. Site and isotope effects on the molecular hydrogen elimination from ethylene have been clearly observed from the photodissociation of ethylene at 157 nm. Experimental results show that there are three different types of molecular elimination processes: 1,1 elimination, 1,2-*cis* elimination, and 1,2-*trans* elimination. Significant differences have been detected between 1,1 elimination and 1,2 eliminations in their kinetic energy distributions. Noticeable difference is also found between 1,2-*cis* elimination and 1,2-*trans* elimination for molecular deuterium elimination. Branching ratios for atomic and molecular hydrogen elimination processes have also been determined for ethylene and its isotopomers. Isotope and site effects on the branching ratios of different molecular elimination channels have been observed. The experimental results are also compared with recent theoretical studies. © 2000 American Institute of Physics. [S0021-9606(00)01345-3]

I. INTRODUCTION

Even though the unimolecular decomposition process of ethylene has been the topic of extensive experimental and theoretical studies for the last few decades, many details of the dissociation processes remains unclear until even today. Previous experimental studies¹⁻⁶ show that the dissociation of ethylene under the excitation of a high energy photon involves four different chemical dissociation channels:



Figure 1 shows the energetic diagram for all possible reaction channels. The first two channels listed above are the molecular hydrogen elimination processes, while the third and the fourth channels are the atomic hydrogen elimination processes. For the atomic hydrogen elimination, there is a triple dissociation channel, in addition to the simple C-H bond rupture process. The dynamics of this triple dissociation channel is a complicated yet interesting phenomenon.

The relative branching ratio for the atomic and molecular hydrogen elimination channel is also an interesting issue.

Previous experimental studies show that any pair of H atoms can participate in molecular elimination, while no clear isotope scrambling has been observed. Molecular hydrogen elimination has been studied in the photodissociation of ethylene at 193 nm excitation.⁷⁻⁹ Site and isotope effects on the dynamics of molecular hydrogen elimination from ethylene have been investigated qualitatively. Molecular elimination from highly excited molecules is an important and also interesting class of unimolecular reactions since it is related not only to simple bond rupture processes but also bond formation processes during dissociation. The chemistry and physics involved in this type of elimination processes are also much more complicated and richer than simple bond rupture dissociation processes. However, there has been lack of systematic studies on the dynamics of the molecular hydrogen elimination so far, especially the precise kinetic and internal energy distributions of the photodissociation products. This is mainly due to the lack of sensitive universal detection methods for molecular hydrogen. Recently, a new molecular beam apparatus has been established in our laboratory.¹⁰ Because of its low background at low masses (mass 1 to mass 4) in the detector in comparison with other similar machines, this apparatus provides us a unique tool to study interesting atomic hydrogen elimination and molecular hydrogen elimination processes.

^{a)} Author to whom correspondence should be addressed. Electronic mail: xmyang@po.iam.s.sinica.edu.tw

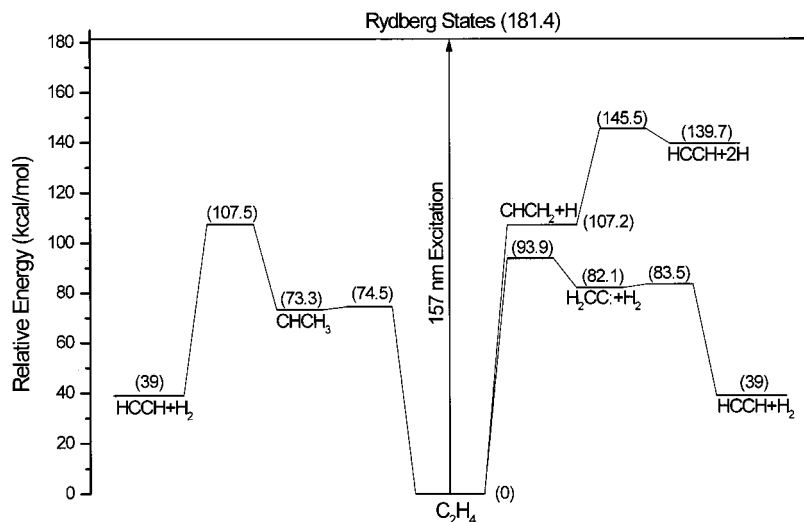


FIG. 1. Energy diagram for all possible dissociation pathways from ethylene at 157 nm.

Molecular elimination process from ethylene can be divided into three types of elimination: 1,1 elimination (11E), 1,2-*cis* elimination (12cE) and 1,2-*trans* elimination (12tE). In each of the three types of elimination, there are two possible pairs of hydrogen atoms for molecular elimination (see Fig. 2). In this work, photodissociation of different ethylene isotopomers at 157 nm are systematically investigated in order to examine the site and isotope effects on the dynamics of molecular hydrogen elimination from ethylene. Atomic hydrogen elimination has also been studied carefully. At 157 nm excitation, the ethylene molecule is mainly excited to the $3p_{x,y,z}$ Rydberg states.¹¹ The equilibrium geometries of the $3p_{x,y,z}$ Rydberg states are all near planar from a recent theoretical calculation (see Fig. 3),¹¹ implying that the 1,2-*cis* and *trans* molecular eliminations could be dynamically different. Recently, we have reported our preliminary results on this interesting topic; site-specific effect on dynamics of the molecular elimination have been reported.¹² Extensive theoretical studies on the photodissociation of ethylene have also been carried out based on a statistical model.¹³⁻¹⁵ In this article, a full report with more careful measurements is presented on this subject.

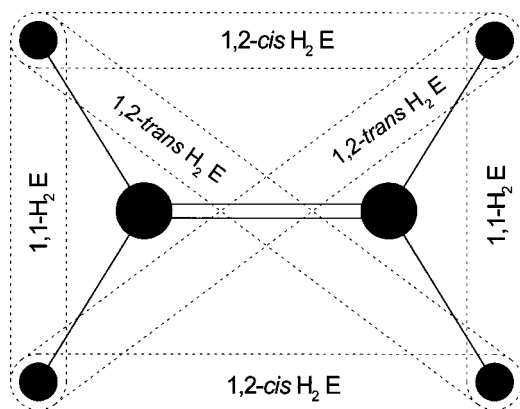


FIG. 2. Site-specific molecular hydrogen elimination processes indicated.

II. EXPERIMENT

Photofragment kinetic spectroscopic technique was used to investigate the photodissociation dynamics of ethylene at 157 nm. The main thrust of this study is to understand the detailed dynamics of the atomic and molecular hydrogen elimination processes from ethylene. The experiment was carried out using a molecular beam apparatus, which consists of two source chambers, a main chamber, and a rotatable universal detector.¹⁶ The most crucial part for this study is the ultraclean detector in the apparatus. The ultrahigh

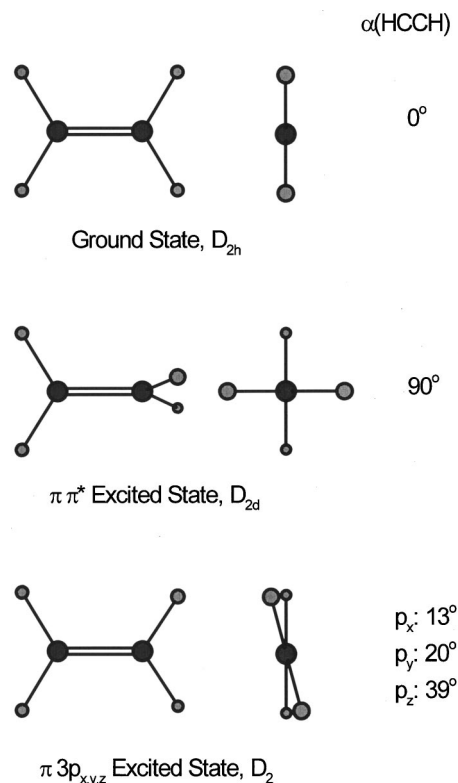


FIG. 3. Molecular geometries of the ground and excited electronic states (from Ref. 11).

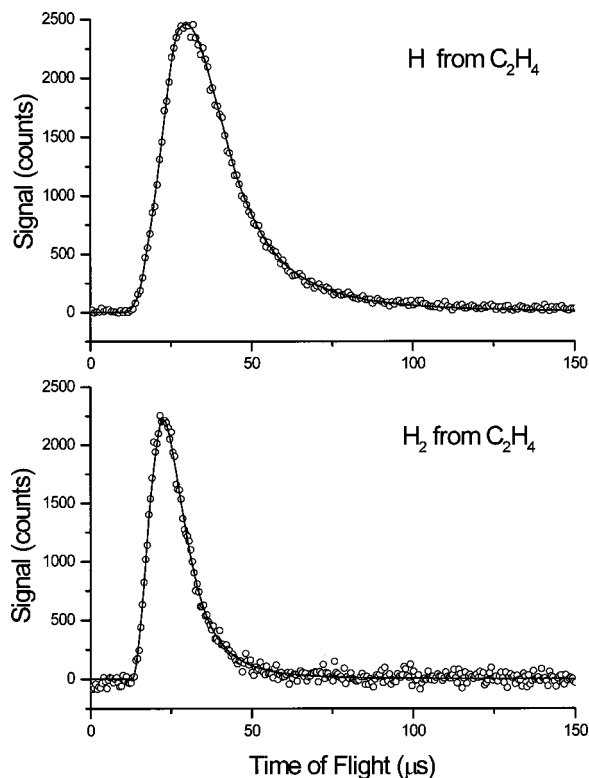


FIG. 4. Experimental and simulated TOF spectra for photodissociation products at $m/e=1,2$ from normal ethylene (C_2H_4) at 157 nm. All spectra were taken by averaging over 25 000 laser shots.

vacuum (1×10^{-12} torr) was maintained during the experiment in the electron-impact-ionization region in order to make the detection of the molecular and atomic hydrogen products much easier. Ethylene and its isotopomers were investigated in order to clarify the sources of the atomic and molecular hydrogen elimination processes.

Totally, five different ethylene isotopomers, normal ethylene (CH_2CH_2), d_4 -ethylene (CD_2CD_2), 1,1- d_2 -ethylene (CD_2CH_2), 1,2-*cis* d_2 -ethylene ($CHDCHD$), and 1,2-*trans* d_2 -ethylene ($CHDCDH$), were obtained commercially for this experimental study. All the samples used here are rated with 99% or better purity. These samples were used without any purification. The light source used in this study was an unpolarized 157 nm laser beam generated by a Lambda Physik LPX 210iF₂ laser with a NOVA tube laser cavity. The repetition rate used in the experiment is 50 Hz and the laser pulse duration is ~ 15 ns. A differentially pumped laser beam path was used, and the vacuum of the laser beam path was $\sim 1 \times 10^{-7}$ Torr or better. In order to avoid multiphoton effects, the 157 nm laser power was attenuated by a mesh to about 1–2 mJ/pulse in the experiment. The laser flux density was also reduced by focusing the laser beam by a MgF₂ lens to a larger spot size of ~ 4 mm \times 4 mm in the interaction region. A pulsed molecular beam was produced by expanding the neat ethylene samples from a solenoid valve (General Valve) through a 0.5 mm diameter orifice. The backing pressure of ethylene and its isotopomers during the experiment was 50 Torr.

Typically, lighter photodissociation products (H and H₂) fly faster so that their residence time in the ionizer is shorter,

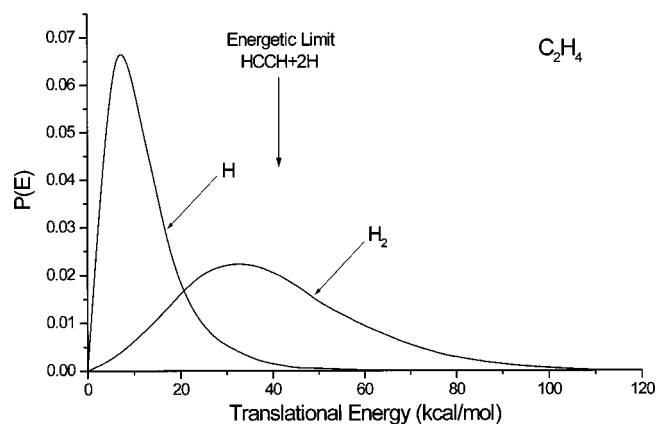


FIG. 5. Kinetic energy distributions obtained for the H and H₂ elimination processes from the simulating the TOF spectra in Fig. 4.

therefore the ionization efficiency of these products is smaller as a result. For H and H₂ products, the ionization efficiency is typically $\sim 10^{-5}$. The laser beam was crossed with the molecular beam perpendicularly at the distance of ~ 5 mm away from the nozzle tip. Such close nozzle-laser distance (higher target density) is used to compensate the low detection efficiency of the lighter fragment. The beam conditions are poorer under these conditions. However, since the H and H₂ products fly much faster than the beam velocity, time-of-flight (TOF) resolution for these products is still acceptable. The photodissociation products pass through a hole of 4 mm diameter on the cold plate near the source chamber wall and enter the main chamber. The products then fly into the detector through a square hole of 4.5 mm \times 4.5 mm on the detector chamber wall. The flight distance (L) of the neutral products was about 285 mm and the detection axis was orthogonal to both the laser beam and the molecular beam. The neutral products were ionized by a Brink-type ionizer,¹⁶ and the length of the ionization region (L) was ~ 13 mm. Ions produced in the ionizer were then focused into the quadrupole mass assembly by some ion optics, mass selected by the quadrupole mass filter (Extrel), and finally counted by a Daly-type ion detector.¹⁶ In this study, the data were accumulated over 2×10^4 – 4×10^5 laser shots depending on the signal-to-noise (S/N) ratios. All experimental conditions such as molecular number density and laser intensity in the interaction region were well controlled in order to make meaningful comparisons of results from different isotopomers. Multiphoton effects and molecular clustering effects were carefully checked.

Product TOF spectra from photodissociation of the ethylene compounds were measured in the laboratory frame. In order to obtain the center-of-mass (CM) kinetic energy distributions $P(E_T)$, the conversions from the laboratory frame to the CM frame are required. The conversions for this study were done by a forward convolution method. Simulations were carried out using a recently developed window-based software package, CMLAB3,¹⁷ which was modified from the previous version, CMLAB2.¹⁸ In this simulation program, a trial $P(E_T)$, and a CM angular distribution (β -parameter) are used to calculate the TOF spectrum for the photofragment at a laboratory (LAB) angle (Θ_{lab}) between the molecular

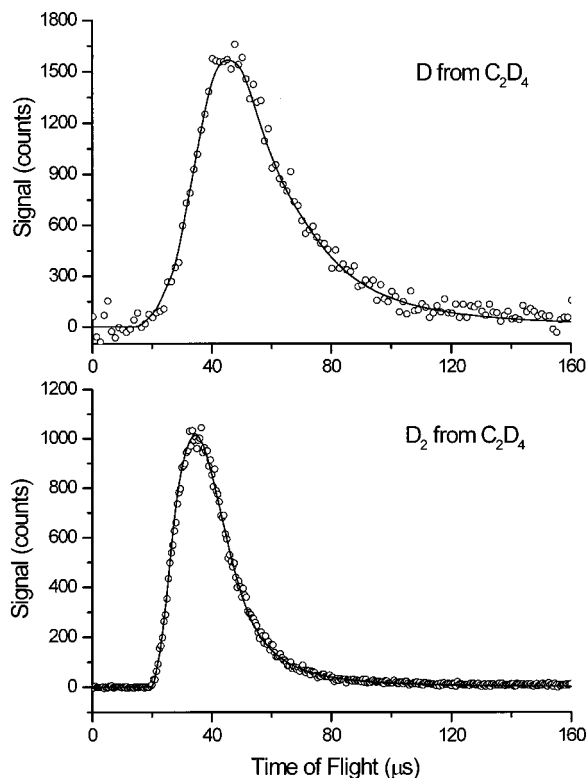


FIG. 6. Experimental and simulated TOF spectra for photodissociation products at $m/e=2,4$ from fully deuterated ethylene (C_2D_4) at 157 nm. All spectra were taken by averaging over 25 000 laser shots.

beam and the detector using the known apparatus parameters and the measured beam velocity distribution (v_{beam}). The calculated TOF spectrum was then compared with the experimental TOF spectrum and the $P(E_T)$ was adjusted point-by-point on the computer screen until satisfactory fit was achieved for the TOF spectrum.

Relative branching ratios of different dissociation channels were calculated by integrating the signals in the CM frame. In order to determine accurately the relative yields of different photodissociation products, detection efficiencies of H_2 , HD, and D_2 were determined by measuring the intensities of the continuous effusive beam consisting of an equimolar mixture of H_2 , HD, and D_2 at $m/e=2, 3$, and 4. Since the total ionization cross sections of H_2 and D_2 are known to be nearly identical,¹⁹ HD is expected to have the same ionization cross section as H_2 and D_2 . From the relative detection efficiencies of H_2 , HD, and D_2 , the detection efficiency of H atom at $m/e=1$ could be estimated since the relative ionization efficiency of H and H_2 was also known.¹⁹

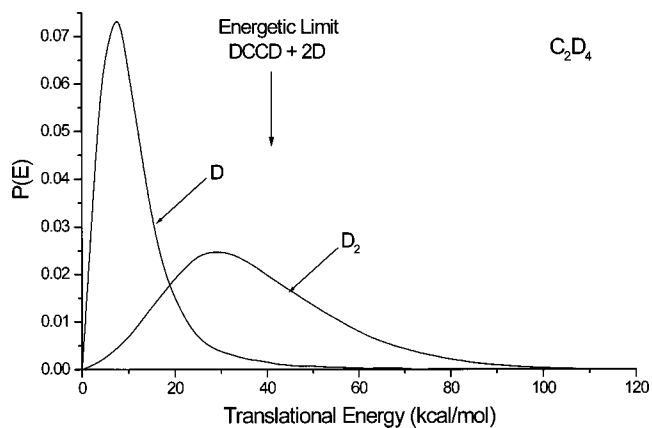


FIG. 7. Kinetic energy distributions obtained for the D and D_2 elimination processes from the simulating the TOF spectra in Fig. 6.

III. RESULTS AND ANALYSES

A. Ethylene (C_2H_4)

TOF spectra of the photodissociation products, H and H_2 , from the normal ethylene at 157 nm, were recorded at the perpendicular direction of the molecular beam using the experimental method described above. Figure 4 shows the TOF spectra at $m/e=1$ (H) and 2 (H_2) from the photodissociation of the normal ethylene. These TOF spectra are simulated using the CMLAB3 program, and the simulated TOF spectra are also shown in Fig. 4. For the H atom elimination, the triple product channel C_2H_2+2H is clearly present since very slow H product is produced above the triple dissociation limit. Figure 5 shows the kinetic energy distributions obtained from simulating the above TOF spectra. In the simulations, the H atom product TOF spectrum is simulated assuming that the H atom products are all from binary dissociation. Even though this way of fitting is approximate, it is helpful to understand the overall characteristics of the H atom elimination. Therefore the kinetic energy distribution obtained for the H atom elimination is for the total H atom products. Atomic elimination processes in work are simulated in this way for all the molecules. From Fig. 5, the H_2 elimination process shows a broad product kinetic energy distribution with its peak at ~ 30 kcal/mol, indicating that the H_2 elimination process has a significant reverse barrier. This is not surprising since H_2 elimination normally has such a reverse barrier. For the H atom elimination, the kinetic energy distribution shows a narrow energy distribution with its peak around 8 kcal/mol. The overall kinetic energy release is quite low for the H atom elimination process. Most of the H

TABLE I. Relative yields of all low mass products from ethylene at 157 nm.

Molecule	H	D	H_2	HD	D_2
C_2H_4	0.56(0.59) ^a	...	0.44(0.41)
C_2D_4	...	0.40(0.53)	0.60(0.47)
1,1 CD_2CH_2	0.32(0.28)	0.15(0.28)	0.20(0.19)	0.23(0.12)	0.10(0.13)
<i>cis</i> -CHDCHD	0.38(0.34)	0.14(0.23)	0.07(0.04)	0.35(0.36)	0.06(0.03)
<i>trans</i> -CHDCDH	0.41(0.33)	0.14(0.22)	0.07(0.04)	0.35(0.38)	0.04(0.03)

^aNumbers in the parentheses are theoretical values from Ref. 14.

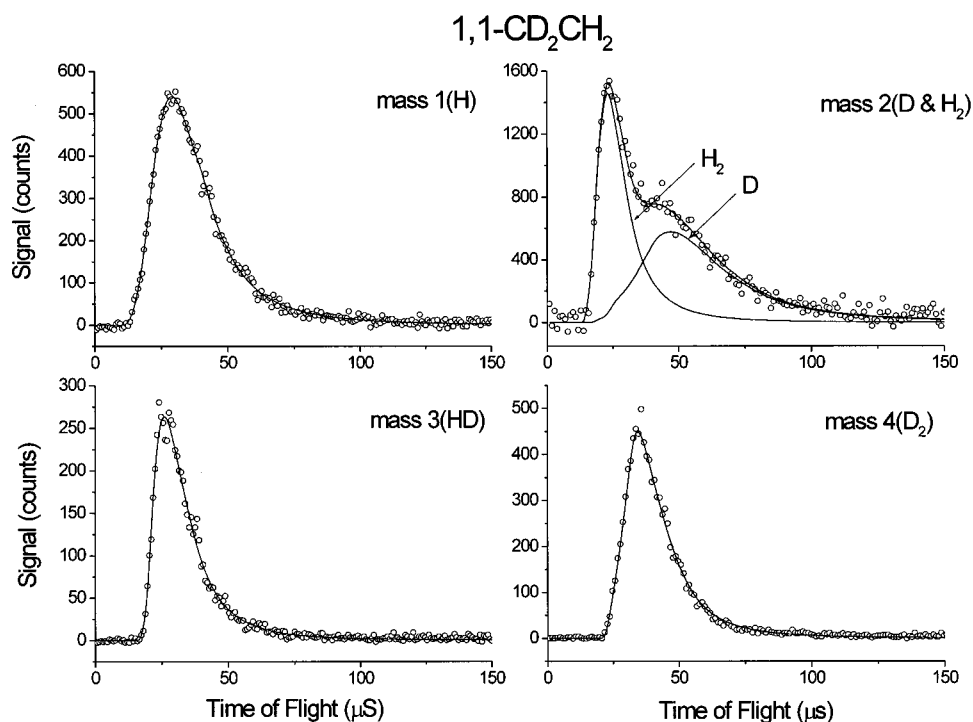


FIG. 8. Experimental and simulated TOF spectra for photodissociation products at $m/e = 1, 2, 3,$ and 4 from 1,1 dideuterated ethylene at 157 nm. All spectra were taken by averaging over 25 000 laser shots.

products actually are produced above the triple dissociation channel limit ($\text{HCCH} + 2\text{H}$), indicating that the dominant H products are likely from the triple dissociation channel.

Using the known relative detection efficiencies and the measured relative signals for the H and H_2 products, branching ratios have also been determined for the two products. The two channels appear to be almost equally important. The results are listed in Table I.

B. Fully deuterated ethylene (C_2D_4)

TOF spectra of the photodissociation products, D and D_2 , from the fully deuterated ethylene at 157 nm were recorded at the perpendicular direction of the molecular beam using the experimental method described above. Figure 6 shows the TOF spectra at $m/e = 2(\text{D})$ and $4(\text{D}_2)$ from the photodissociation of the normal ethylene. These TOF spectra are fitted using the CMLAB3 program, and the simulated TOF spectra are also shown in Fig. 6. Figure 7 shows the kinetic energy distributions obtained from simulating the above TOF spectra. Similar to the analysis of the normal ethylene data, the TOF spectrum for the D atom products was simulated as a binary dissociation process. This is an approximate way to extract information for the H atom elimination process. The kinetic energy distributions for the D and D_2 elimination processes from C_2D_4 are very similar to that for the H and H_2 elimination from C_2H_4 , indicating the dynamics of the two processes in the two molecules are very similar to each other. Using the relative detection efficiencies for the apparatus and the measured relative signals for the D and D_2 products, branching ratios have been determined for the two product channels. In comparison with the C_2H_4 results, the molecular deuterium from C_2D_4 is more important than the molecular

hydrogen elimination from C_2H_4 . Therefore isotope effect on branching ratios is clearly present. The branching ratios are listed in Table I.

C. 1,1-dideuterated ethylene (CD_2CH_2)

TOF spectra of the photodissociation products at mass 1(H), 2(H_2 &D), 3 and 4(D_2) from 1,1-dideuterated ethylene at 157 nm using the experimental method described above were recorded. Figure 8 shows the TOF spectra at $m/e = 1(\text{H}), 2(\text{D}\&\text{H}_2), 3$ and $4(\text{D}_2)$ from the photodissociation of the 1,1-dideuterated ethylene. These TOF spectra are simulated using the CMLAB3 program, and the simulated TOF spectra are also shown in Fig. 8. Similar to the above analysis, the H and D atom products are simulated assuming these products are from a binary dissociation. Figure 9 shows the kinetic energy distributions obtained for all the product chan-

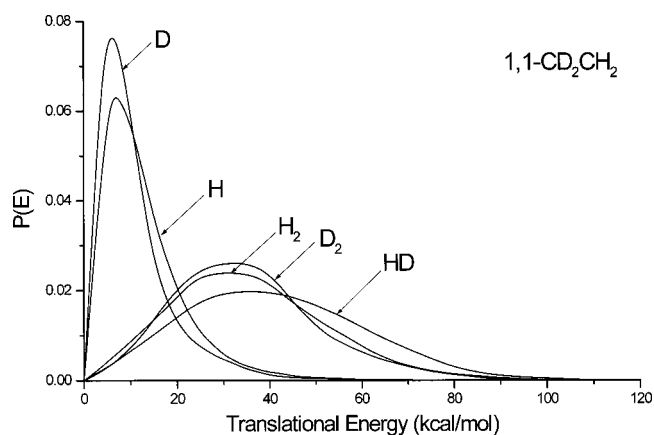


FIG. 9. Kinetic energy distributions obtained for the H, D, H_2 , HD, and D_2 elimination processes from the simulating the TOF spectra in Fig. 8.

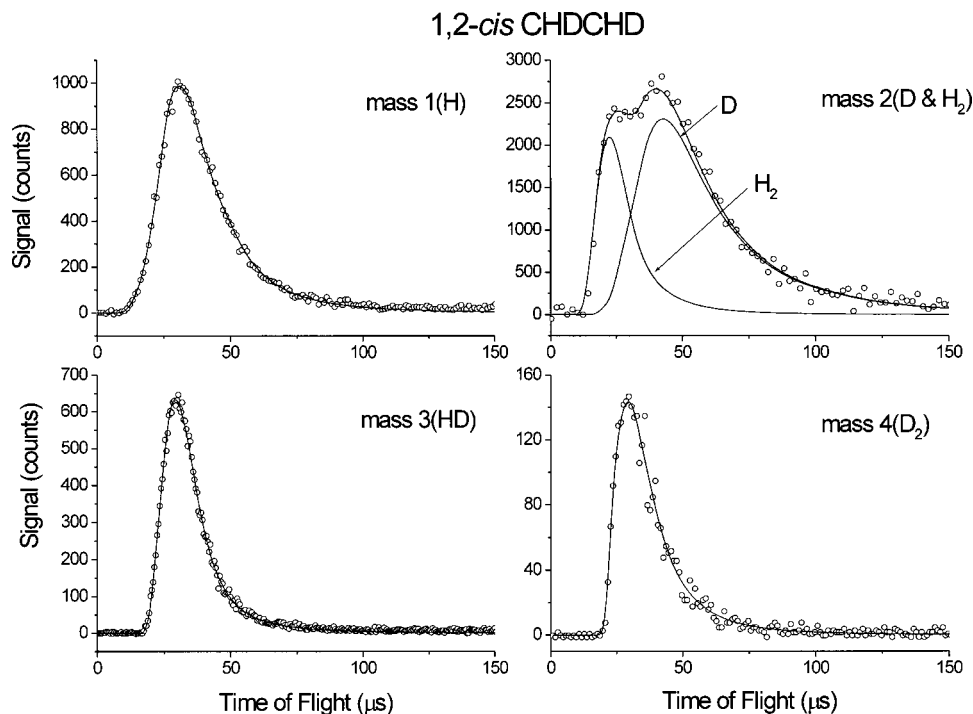


FIG. 10. Experimental and simulated TOF spectra for photodissociation products at $m/e = 1, 2, 3,$ and 4 from $1,2$ -*cis* dideuterated ethylene at 157 nm. All spectra were taken by averaging over $25\,000$ laser shots.

nels from simulating the above TOF spectra. From Fig. 9, it is clear that the H and D processes have similar kinetic energy distributions, while H_2 , HD, and D_2 elimination processes also have similar distributions. Noticeable differences were found for the HD and D_2 eliminations from CD_2CH_2 . Since the D and H_2 signals are overlapped in some degree, the kinetic energy distributions obtained for the two processes should have larger error bars than those of other processes. Similarly, branching ratios have been determined for all the product channels in the same way used above. The branching ratios determined are listed in Table I. Notice that H atom product is about twice that of the D atom product, while H_2 and HD are about twice that of the D_2 product. This implies that large isotope effects are present in the atomic and molecular hydrogen elimination processes.

D. $1,2$ -*cis* dideuterated ethylene (CHDCHD)

TOF spectra of the photodissociation products at masses $1, 2, 3, 4$ from $1,2$ -*cis* dideuterated ethylene at 157 nm were recorded. Figure 10 shows the TOF spectra at $m/e = 1$ (H), 2 (D & H_2), 3 and 4 (D_2) from $1,2$ -*cis* dideuterated ethylene. These TOF spectra are simulated in exactly the same way used in the above section. The simulated TOF spectra are shown in Fig. 10. Also similar to the above analysis, the H and D products are treated as products from a binary dissociation. Figure 11 shows the kinetic energy distributions obtained for all product channels from simulating the above TOF spectra. Similarly, using the known relative detection efficiencies and the measured relative signals for the H, D, H_2 , HD, and D_2 products, branching ratios have also been determined for these product channels, which are listed in Table I. The relative yields of the H and D products from this isotopomer are very similar to that of CH_2CD_2 , whereas those relative of H_2 , HD, and D_2 are very different from that

of CH_2CD_2 . Similar to CH_2CD_2 , isotope effects are present in the atomic and molecular elimination processes.

E. $1,2$ -*trans* dideuterated ethylene (CHDCDH)

TOF spectra of the photodissociation products at masses $1, 2, 3,$ and 4 from $1,2$ -*trans* dideuterated ethylene at 157 nm were recorded. Figure 12 shows the TOF spectra at $m/e = 1$ (H), 2 (D & H_2), 3 and 4 (D_2) from $1,2$ -*trans* dideuterated ethylene. These TOF spectra are simulated in exactly the same way used in the above section. The simulated TOF spectra are shown in Fig. 12. Also similar to the above analysis, the H and D products are treated as products from a binary dissociation. Figure 13 shows the kinetic energy distributions obtained for all product channels from simulating the above TOF spectra. Similarly, using the known relative detection efficiencies and the measured relative signals for

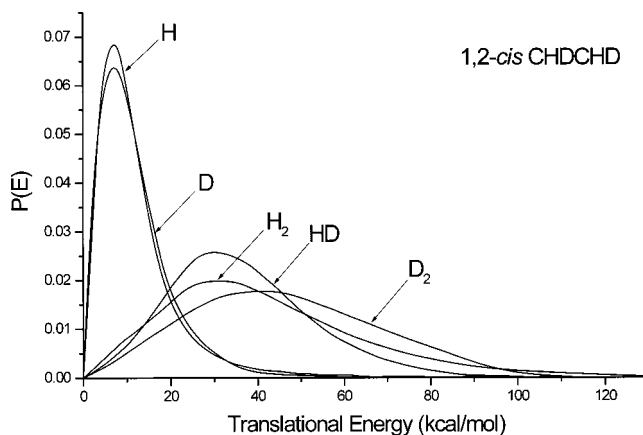


FIG. 11. Kinetic energy distributions obtained for the H, D, H_2 , HD, and D_2 elimination processes from the simulating the TOF spectra in Fig. 10.

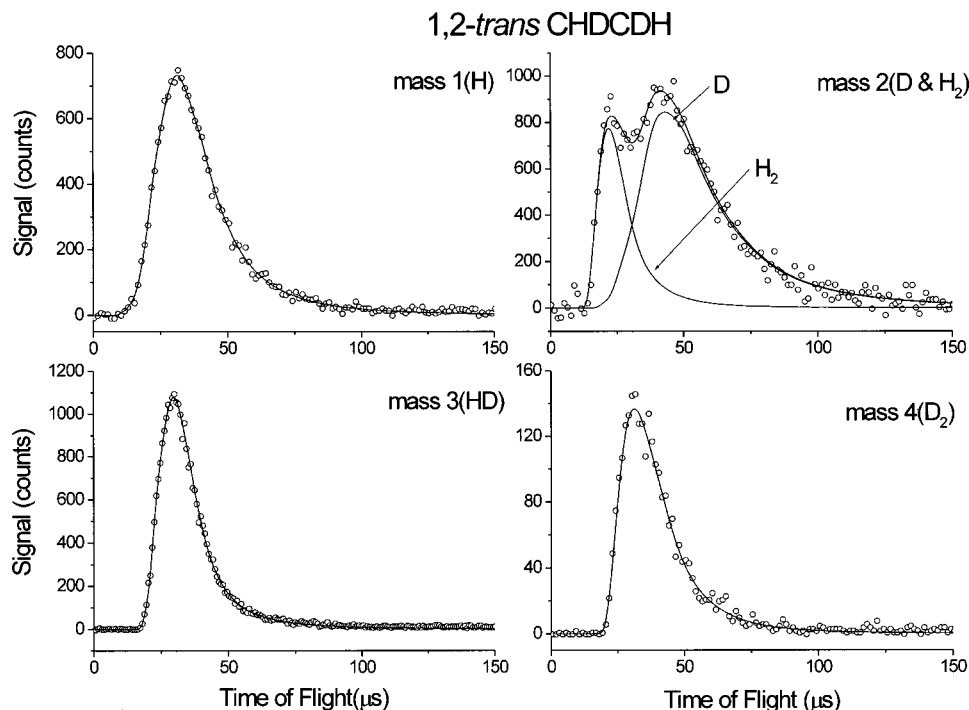


FIG. 12. Experimental and simulated TOF spectra for photodissociation products at $m/e=1, 2, 3,$ and 4 from $1,2$ -*trans* dideuterated ethylene at 157 nm. All spectra were taken by averaging over $25\,000$ laser shots.

the H, D, H_2 , HD, and D_2 products, branching ratios have been determined for all the product channels, which are listed in Table I. Notice that the relative yields of the H and D products from this isotopomer are very similar to that of CH_2CD_2 and $1,2$ -*cis* CHDCDH, whereas those relative of H_2 , HD, and D_2 are very different from that of CH_2CD_2 but similar to that of $1,2$ -*cis* CHDCDH.

F. Site and isotope effects on the atomic and molecular hydrogen eliminations

In order to know whether a meaningful comparison can be made across all isotopomers, total photodissociation signals (from $m/e=1$ to 4) from the three dideuterated ethylene isotopomers were compared. Without considering the transformation (LAB-to-CM frame) differences between different isotopomers, which are considered to be small since the shape of the total signal of the three compounds are quite similar, the integrated signals from the three dideuterated ethylenes were all within 5% of each other, indicating that the photodissociation of three deuterated ethylene molecules can be compared quantitatively. It is necessary to point out that the product angular anisotropy in the dissociation processes might also cause some small differences in the branching ratios. However, this should not cause any significant difference because unpolarized laser source is used in the experiment. In addition, experimental results here show that molecular hydrogen elimination from ethylene most likely occurs on the ground potential surface through internal conversion from the initially excited state. This would likely wash out the product angular anisotropy in the dissociation processes. The original geometry of the ethylene molecule also points to a small angular anisotropy parameter for molecular elimination even if it is a direct and fast dissociation process.

Since dissociative ionization of the molecular hydrogen product can be neglected, the signals observed at $m/e=1,2,3,4$ should be the photodissociation products of H, H_2 &D, HD, and D_2 , respectively. By fitting these TOF spectra at $m/e=2,3,4$ from all three isotopomers, the kinetic energy distributions and yields for each channel have been determined. From Fig. 2, the H_2 and D_2 eliminations from all three deuterated ethylenes are clearly site-specific. The H_2 and D_2 eliminations from $1,2$ -*trans* CHDCDH are all due to site-specific $1,2$ -*trans* elimination (12tE), the H_2 and D_2 eliminations from $1,2$ -*cis* CHDCDH are all due to site-specific $1,2$ -*cis* elimination (12cE), and the H_2 and D_2 eliminations from $1,1$ CH_2CD_2 are all due to site-specific $1,1$ elimination (11E). While the H_2 and D_2 eliminations are site-specific, the HD eliminations from the three deuterated compounds are the combination of two different site eliminations (see Fig. 2). As shown in Fig. 2, the HD elimination from

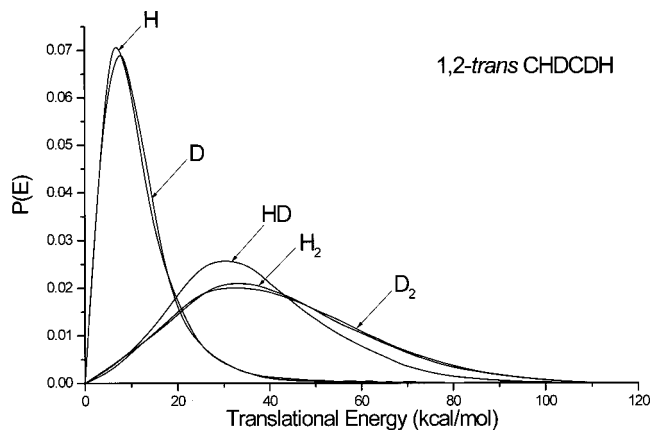


FIG. 13. Kinetic energy distributions obtained for the H, D, H_2 , HD, and D_2 elimination processes from the simulating the TOF spectra in Fig. 12.

TABLE II. Relative yields of specific site H₂, HD, and D₂ eliminations.

Specific site elimination	D ₂	HD	H ₂
1,2- <i>trans</i> elimination (12tE)	1.00	1.64	2.03
1,2- <i>cis</i> elimination (12cE)	1.68	1.60	2.02
1,1 elimination (11E)	2.81	3.37	5.65

1,2-*trans* CHDCHD is the combination of the 1,1 HD elimination and the 1,2-*cis* HD elimination; the HD elimination from 1,2-*cis* CHDCHD is the combination of the 1,1 HD elimination and the 1,2-*trans* HD elimination; and the HD elimination from 1,1 CH₂CD₂ is the combination of the 1,2-*cis* HD elimination and the 1,2-*trans* HD elimination.

Since the H₂ and D₂ elimination processes are site-specific, the relative yields listed for the H₂ and D₂ eliminations in Table I are also site-specific. The HD elimination from each ethylene isotopomer, however, is a combination of two specific site eliminations. Therefore the total HD yields listed in Table I are not site-specific. In order to determine the site-specific HD yield, the total HD yield from each deuterated ethylene can be viewed as the summation of the two site-specific HD yields, and each specific site HD yield from different deuterated ethylene molecules is assumed to be the same:

$$Y_{\text{HD}}(1,2=\textit{trans} \text{ CHDCHD}) = 2y_{\text{HD}}(11\text{E}) + 2y_{\text{HD}}(12\text{cE}), \quad (5)$$

$$Y_{\text{HD}}(1,2=\textit{cis} \text{ CHDCHD}) = 2y_{\text{HD}}(11\text{E}) + 2y_{\text{HD}}(12\text{tE}), \quad (6)$$

$$Y_{\text{HD}}(1,1 \text{ CH}_2\text{CD}_2) = 2y_{\text{HD}}(12\text{cE}) + 2y_{\text{HD}}(12\text{tE}), \quad (7)$$

where Y_{HD} is the total yield of HD elimination, and y_{HD} is the yield of site-specific HD elimination. Solving the above equations, the relative yields for the site-specific HD eliminations can be obtained. Table II lists the relative yields of the H₂, HD, and D₂ site-specific elimination processes.

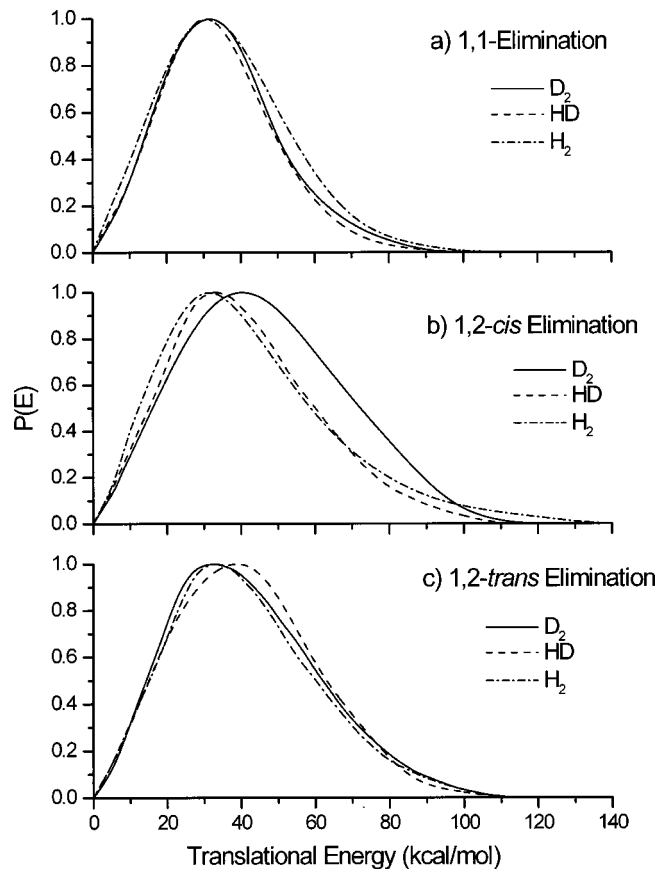
The kinetic energy distributions for the site-specific eliminations of H₂, HD, and D₂ are also obtained through the simulation using the CMLAB3 program. Since the H₂ and D₂ eliminations are all site-specific, the kinetic energy distributions obtained for these processes are also all site-specific. However, the kinetic energy distributions for site-specific HD eliminations from the three dideuterated compounds can be obtained using a similar method to the calculations of the site-specific HD yields. Here, the kinetic energy distribution of the HD elimination from a dideuterated ethylene can be viewed as the summation of the contributions of the two site-specific HD elimination:

$$P_{12\text{t}}(E) = 2p_{11\text{E}}(E) + 2p_{12\text{cE}}(E), \quad (8)$$

$$P_{12\text{c}}(E) = 2p_{11\text{E}}(E) + 2p_{12\text{tE}}(E), \quad (9)$$

$$P_{11}(E) = 2p_{12\text{tE}}(E) + 2p_{12\text{cE}}(E), \quad (10)$$

where $P_{12\text{t}}(E)$, $P_{12\text{c}}(E)$, and $P_{11}(E)$ are the kinetic energy distribution for the total HD elimination from 1,2-*trans* CHDCHD, 1,2-*cis* CHDCHD, and 1,1 CH₂CD₂, respectively, while $p_{12\text{tE}}(E)$, $p_{12\text{cE}}(E)$, and $p_{11\text{E}}(E)$ are the kinetic distribution for each specific site HD elimination: 1,2-*trans* elimination, 1,2-*cis* elimination, and 1,1 elimination, respec-

FIG. 14. Site effect on the $P(E)$ s for D₂, HD, and H₂ elimination.

tively. From the measured kinetic distributions $P_{12\text{t}}(E)$, $P_{12\text{c}}(E)$, and $P_{11}(E)$, the kinetic energy distributions $p_{12\text{tE}}(E)$, $p_{12\text{cE}}(E)$ and $p_{11\text{E}}(E)$ for the site specific HD elimination can be determined by solving the above equations. The specific site effect on the kinetic energy distribution of the H₂, HD, and D₂ elimination is shown in Fig. 14. For convenience of comparison, all kinetic energy distributions shown in these figures are normalized to the same height.

The isotope effect on the kinetic energy distribution is also quite interesting (see Fig. 15). For the 1,1 molecular hydrogen elimination channel, the kinetic energy distributions for H₂, HD, D₂ are almost exactly the same (see Fig. 15), implying that the isotope effect on the dynamics of the 1,1 elimination channel are very small. However, the isotope effect on the kinetic energy distributions for the four center elimination channels, especially the 1,2-*cis* elimination, is much more significant. From Table II, it is also obvious to see that the relative yields for any specific site elimination increase as the eliminated species (D₂, HD, and H₂) becomes lighter.

From the kinetic energy distributions and yields for the specific site H₂, HD, and D₂ elimination (see Fig. 14 and Table II), it is very clear that the 1,1, 1,2-*cis*, and 1,2-*trans* D₂ elimination processes show significantly differences in their kinetic energy distributions, indicating that the dynamics of D₂ elimination from different sites are quite different.

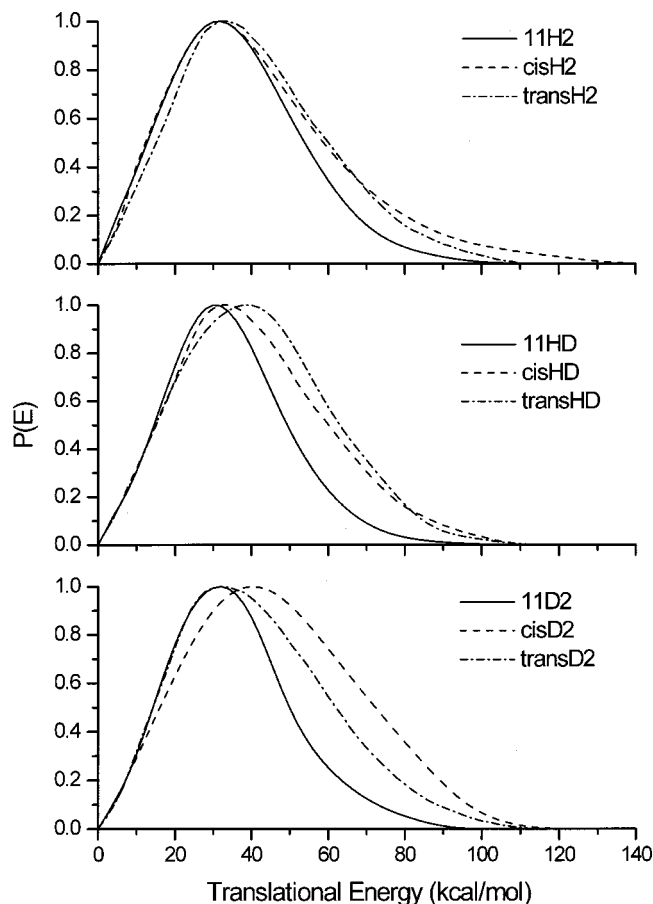


FIG. 15. Isotope effect on the $P(E)$ s for specific site elimination.

The difference between the 1,2-*cis* and 1,2-*trans* D_2 elimination is especially interesting because all previous studies at different wavelength excitations show no differences between these two microchannels. The HD eliminations from different sites also show some differences in their kinetic energy distributions. For the H_2 elimination processes, however, there is no obvious difference between the 1,2-*cis* and 1,2-*trans* H_2 eliminations. From theoretical studies, the four-center molecular hydrogen elimination requires a 1,2 hydrogen atom migration. The transition state of the 1,2 elimination is believed to be the so-called ethylidene radical ($:CHCH_3$).^{20–23,13–15} Recent theoretical studies on the ethylene photodissociation show that the structures of the transition state of the 1,2-*trans* and the 1,2-*cis* elimination processes are slightly different.¹⁴ This will certainly cause some difference in the 1,2-*cis* and 1,2-*trans* elimination processes. The main difference shown in the dynamics of 1,2-*cis* and 1,2-*trans* eliminations could not, however, be solely explained by the differences in the transition states. Other dynamical processes such as 1,2 concerted molecular hydrogen elimination, which does not require 1,2 hydrogen atom shift, might be responsible for the main difference between the 1,2-*cis* and 1,2-*trans* molecular hydrogen eliminations. It is conceivable that the concerted molecular hydrogen eliminations from *cis* and *trans* configurations might be quite different because the migration distances between the two hydrogen atoms are significantly different in the two type

TABLE III. Averaged kinetic energy releases from photodissociation of ethylene at 157 nm.

Molecule	H	D	H_2	HD	D_2
C_2H_4	12.4	...	39.8
C_2D_4	...	11.2	37.4
1,1 CD_2CH_2	12.9	11.5	35.6	41.8	35.2
<i>cis</i> -CHDCDH	12.3	12.0	39.3	36.1	45.5
<i>trans</i> -CHDCDH	11.9	11.5	40.4	36.2	40.4

eliminations in which tunneling effect might be important.

Recent theoretical studies also showed that conical intersections might be important in this system,^{24–26} indicating that internal conversion from the excited electronic state to the ground electronic state might be very efficient. In addition, the theoretical results also indicate that *cis*–*trans* isomerization in ethylene can also be promoted through conical intersections. From the difference observed between the 1,2-*cis* and 1,2-*trans* H_2 elimination in this work, it is likely that *cis*–*trans* isomerization should not be much faster than the dissociation process. In other words, isomerization should not be complete before dissociation.

From Table I, there is a clear isotope effect on the branching ratios of the atomic hydrogen elimination. However, kinetic energy distributions for atomic hydrogen (or deuterium) eliminations are all very similar, indicating there is no obvious isotope effect on the dynamics of the atomic hydrogen elimination process.

G. Comparisons with theoretical calculations

Recently, Chang *et al.* has calculated both the product branching ratios and the kinetic energy distributions for the photodissociation of ethylene and its isotopomers at 157 nm and other wavelengths using an RRKM model.¹⁵ The calculated branching ratios are also listed in Table I in comparison with the experimental values. From Table I, the overall agreement between the calculated branching ratios and experimental results are quite good, indicating that the RRKM picture is quite good for the photodissociation of ethylene at 157 nm. However, there are quantitative differences between the calculated and measured branching ratios. The atomic hydrogen elimination channels are always overestimated in the theoretical calculations, and the D elimination channel is always overestimated relative to the H atom elimination from the three deuterated ethylene compounds. In the calculations, the difference between the 1,1 molecular hydrogen elimination and the 1,2 molecular hydrogen elimination is quite close to the experimental results, indicating that the theoretical model is quite good. However, the difference between the 1,2-*cis* and 1,2-*trans* molecular hydrogen eliminations observed in the experiments do not show up in the theoretical calculations, indicating that the RRKM model seems to be inadequate to predict this difference.

Averaged kinetic energy releases have been determined for the kinetic energy distributions for different reaction channels. The results are listed in Table III. From these results, the averaged kinetic energy releases (~ 12 kcal/mol) for the atomic hydrogen elimination processes are always a

little bit higher than the calculated values (~ 9 kcal/mol). For the molecular hydrogen eliminations, the calculated averaged kinetic energy release for the 1,1 elimination is about 22 kcal/mol, which is significantly lower than the measured value (~ 35 kcal/mol), while the calculated value for the 1,2 elimination process is about 70 kcal/mol, which is significantly higher than the observed value (~ 40 kcal/mol). These results indicate that the RRKM theoretical model is clearly inadequate to describe the product kinetic energy distributions even though the model is quite good in predicting the branching ratios for different dissociation channels. It seems that the two dynamical pathways (1,1 and 1,2 elimination processes) are somewhat mixed so that the actual barrier for the 1,1 H_2 elimination is substantially higher, while that for the 1,2 H_2 elimination is significantly lower. Clearly such mixing is not complete, thus certain site-specificity is maintained in the system. The cause of such dynamical mixing is an interesting issue. Since it is very likely that conical intersections are involved in the nonadiabatic processes from the excited state to the ground state, these conical intersections could play an important role in the dynamical mixing. It is conceivable that the ethylene molecules receive strong forces during the transition period through the conical intersection, which force the molecules to go to different dynamical pathways as statistical models predict. This could also explain the non-RRKM behaviors of the product energy depositions in the molecular hydrogen elimination processes. More detailed studies on the role of conical intersections in the ethylene photodissociation process will be helpful to clarify these issues. The above comparisons also show that a fully statistical model could not fully describe the photodissociation process of the ethylene molecule at 157 nm. However, some characteristics of the ethylene photodissociation can be described by an RRKM statistical model, indicating that the process is probably at least partially randomized.

IV. CONCLUSIONS

Photodissociation of five ethylene isotopomers at 157 nm has been studied using a molecular beam apparatus. From this study, complete and interesting information on the site and isotope effects on the molecular hydrogen elimination processes from ethylene has been derived. Using the new improved experimental technique, dynamical differences between different microchannels of molecular hydrogen elimination processes from ethylene have also been detected. Site and isotopic effects on the molecular hydrogen elimination processes have been clearly observed. From the experimental results in this work, atomic hydrogen elimination and molecular hydrogen elimination from ethylene are almost equally important. Atomic hydrogen elimination

mostly results from triple dissociation, while molecular hydrogen elimination should be essentially a binary dissociation process. The branching between the atomic hydrogen and molecular hydrogen does not change significantly for different isotopomers. Comparisons with recent theoretical calculations show that a statistical RRKM model could not fully describe the ethylene photodissociation at 157 nm, indicating this system is not fully statistical. The results of this work provide a good example of site-specific molecular elimination processes.

ACKNOWLEDGMENTS

This work is supported by the National Research Council and Academia Sinica of the Republic of China. Financial Support from the China Petroleum Company is also greatly appreciated. We are very grateful to Dr. A. H. H. Chang, Professor A. M. Mebel, and Professor S. H. Lin for many helpful discussions.

- ¹M. Sauer, Jr. and L. M. Dorfman, *J. Chem. Phys.* **35**, 497 (1961).
- ²R. A. Back and D. W. L. Griffiths, *J. Chem. Phys.* **46**, 4839 (1967).
- ³H. Hara and I. Tanaka, *Bull. Chem. Soc. Jpn.* **46**, 3012 (1973); **47**, 1543 (1974).
- ⁴P. Ausloos and R. Gordien, Jr., *J. Chem. Phys.* **36**, 5 (1962).
- ⁵H. Okabe and J. R. McNesby, *J. Chem. Phys.* **36**, 601 (1962).
- ⁶A. B. Callear and R. J. Cvetanovic, *J. Chem. Phys.* **24**, 873 (1956).
- ⁷B. A. Balko, J. Zhang, and Y. T. Lee, *J. Chem. Phys.* **97**, 935 (1992).
- ⁸A. Stowlow, B. A. Balko, E. F. Cromwell, J. Zhang, and Y. T. Lee, *J. Photochem. Photobiol., A* **62**, 285 (1992).
- ⁹E. F. Cromwell, A. Stowlow, M. J. J. Vrakking, and Y. T. Lee, *J. Chem. Phys.* **97**, 4029 (1992).
- ¹⁰J. J. Lin, D. W. Hwang, S. Harich, Y. T. Lee, and X. Yang, *Rev. Sci. Instrum.* **69**, 1642 (1998).
- ¹¹A. M. Mebel, Y. T. Chen, and S. H. Lin, *J. Chem. Phys.* **105**, 9007 (1996).
- ¹²J. J. Lin, D. W. Hwang, S. Harich, Y. T. Lee, and X. Yang, *J. Chem. Phys.* **109**, 2979 (1998).
- ¹³A. H. H. Chang, A. M. Mebel, X. Yang, S. H. Lin, and Y. T. Lee, *Chem. Phys. Lett.* **287**, 301 (1998).
- ¹⁴A. H. H. Chang, A. M. Mebel, X. Yang, S. H. Lin, and Y. T. Lee, *J. Chem. Phys.* **109**, 2748 (1998).
- ¹⁵A. H. H. Chang, A. M. Mebel, X. Yang, S. H. Lin, and Y. T. Lee, *J. Chem. Phys.* **110**, 10810 (1999).
- ¹⁶J. J. Lin, D. W. Hwang, S. Harich, Y. T. Lee, and X. Yang, *Rev. Sci. Instrum.* **69**, 1642 (1998).
- ¹⁷S. Harich, Ph.D. thesis, University of California, Santa Barbara, CA, 1999.
- ¹⁸X. Zhao, Ph.D. thesis, University of California, Berkeley, CA, 1988; J. D. Myers, Ph.D. thesis, University of California, Berkeley, CA, 1992.
- ¹⁹H. Tawara and T. Kato, *At. Data Nucl. Data Tables* **36**, 167 (1987).
- ²⁰E. M. Evleth and A. Sevin, *J. Am. Chem. Soc.* **103**, 7414 (1981).
- ²¹J. D. Goddard, *Chem. Phys. Lett.* **83**, 312 (1981).
- ²²G. J. Collin, *Adv. Photochem.* **14**, 135 (1988).
- ²³K. Raghachari, M. J. Frisch, J. A. Pople, and P. V. R. Schleyer, *Chem. Phys. Lett.* **85**, 145 (1982).
- ²⁴I. Ohmine, *J. Chem. Phys.* **83**, 2348 (1985).
- ²⁵L. Freund and M. Klessinger, *Int. J. Quantum Chem.* **70**, 1023 (1998).
- ²⁶M. Ben-Nun and T. J. Martinez, *Chem. Phys. Lett.* **298**, 57 (1998).